

Information-Theoretic Measurements of Coupling between Structure and Dynamics in Glass Formers

Robert L. Jack,¹ Andrew J. Dunleavy,^{2,3,4} and C. Patrick Royall^{2,3,5}

¹*Department of Physics, University of Bath, Bath BA2 7AY, United Kingdom*

²*HH Wills Physics Laboratory, Tyndall Avenue, Bristol BS8 1TL, United Kingdom*

³*School of Chemistry, University of Bristol, Cantock Close, Bristol BS8 1TS, United Kingdom*

⁴*Bristol Centre for Complexity Sciences, Bristol BS8 1TW, United Kingdom*

⁵*Centre for Nanoscience and Quantum Information, Tyndall Avenue, Bristol BS8 1FD, United Kingdom*

(Received 28 February 2014; published 28 August 2014)

We analyze connections between structure and dynamics in two model glass formers, using the mutual information between an initial configuration and the ensuing dynamics to compare the predictive value of different structural observables. We consider the predictive power of normal modes, locally favored structures, and coarse-grained measurements of local energy and density. The mutual information allows the influence of the liquid structure on the dynamics to be analyzed quantitatively as a function of time, showing that normal modes give the most useful predictions on short time scales while local energy and density are most strongly predictive at long times.

DOI: 10.1103/PhysRevLett.113.095703

PACS numbers: 64.70.Q-, 05.40.-a

As supercooled liquids approach their glass transitions, structural relaxation slows down dramatically, but molecular configurations remain disordered and apparently random [1,2]. However, computer simulations [3–8] and experiments [9,10] show that liquid structure and dynamical relaxation are correlated in these systems, as predicted (or assumed) in several theories [11–18]. Correlations between structure and dynamics can be demonstrated at a microscopic level [3–8], by exploiting the dynamically heterogeneous nature of glassy relaxation [19]. That is, individual particles have different propensities for motion [3], depending on local structure. Here, we use *information theory* [20] to analyze the strength of these correlations, by measuring the extent to which structural measurements can be used to *predict* particle dynamics at subsequent times. This quantitative analysis provides a stringent test of proposed causal links between structural features and slow dynamics. In two model glass formers, we find that coarse-grained measurements of energy and density [21–23] give the most predictive information for long times. In one of the models, vibrational modes [4–6,17] are strongly correlated with motion on relatively short time scales. Compared to these effects, the correlation between dynamics and low energy (or low enthalpy) local structures is relatively weak.

We consider the Kob-Andersen (KA) mixture of Lennard-Jones particles [24], and an equimolar five-component hard sphere (HS) mixture, which mimics colloidal suspensions [25]. Both systems contain particles of different sizes, with the diameter of the largest particles being $\sigma = 1$ (which sets the unit of length). The KA system evolves with overdamped (Monte Carlo) dynamics as in [26]; we focus on a temperature $T = 0.5$ and density $\rho = 1.2$. The HS system evolves by event-driven molecular dynamics [27]; we consider

volume fractions ϕ in the range 0.52–0.58. In both systems, we use Δt to indicate the fundamental unit of time. The relaxation at the state points that we consider is up to 3 decades slower than relaxation in the high-temperature or low-density regime, where it is of order Δt (in both systems). Further system details are given in the Supplemental Material [28].

To characterize particle dynamics in these systems, we define the dynamical propensity [3] of particle i as $\mu_{i,t} = \langle |\mathbf{r}_i(t) - \mathbf{r}_i(t_0)|^2 \rangle_{\text{iso}}$, where $\mathbf{r}_i(t)$ is the particle position at time t , and the isoconfigurational average is calculated over many independent dynamical simulations, all with the same initial particle positions but with independent random initial velocities (and independent stochastic dynamics in the KA system). The role of the “lag time” t_0 is discussed in Supplemental Material [28]: we take $t_0 \approx 0.1\Delta t$. We use s_i to denote a structural measurement at time $t = 0$, which depends in general on particle i and all particles in its vicinity. To quantify the strength of the correlation between s_i and the dynamical propensity $\mu_{i,t}$, we use mutual information (MI) measurements [20]. The MI is defined as

$$I_t(\mu; s) = \sum_s \int d\mu p_t(\mu, s) \log_2 \frac{p_t(\mu, s)}{p_t(\mu)p(s)}, \quad (1)$$

where $p_t(\mu, s)$ is the joint probability distribution of μ and s , while $p_t(\mu)$ and $p(s)$ are its marginal distributions. In Eq. (1), s_i takes discrete values: for continuous observables s_i , the sum over s is replaced by an integral.

The MI gives “the average amount of information about the propensity μ_{it} that is provided by a measurement of s_i ”. Since s_i depends only on the initial condition, the MI

measures *predictive* information. The MI may be evaluated for any structural observable s_i , and it makes no assumptions on the nature of the correlation between $\mu_{i,t}$ and s_i . As such, it represents a generally applicable figure of merit for comparing the influence on dynamics of different structural measures, going beyond previous comparisons of snapshots [3–6,21,23] or analyses of selected subsets of particles [7,8]. The use of (1) to measure information [20] is similar to the use of entropy as a measure of disorder in statistical mechanics, with the role of disorder being taken by the variation in propensity between different particles. Particles with the same value of s_i typically have less variation in their propensity, so specifying s_i reduces the variation in $\mu_{i,t}$, just as introducing a constraint in statistical mechanics reduces the entropy [36]. The MI is equivalent to this entropy reduction. Information is measured in bits, with one bit corresponding to a reduction in entropy of $k_B \ln 2$. Our procedure for estimating MI is described in the Supplemental Material [28]: the method ensures as far as possible that we obtain $I_t(\mu; s) = 0$ if μ and s are independent; it also provides an estimate of the numerical uncertainty in the MI. For some other recent applications of MI measurements in glassy systems, see [37–41].

To illustrate our use of MI, let s_i be the type (A or B) of particle i in the KA system. The different types have different dynamical relaxation so knowledge of the particle type provides predictive information about particle dynamics. In Supplemental Material [28], we show that measuring a particle’s type provides between 0.1 and 0.7 bits of information about its propensity $\mu_{i,t}$, depending on the time t . This value is a useful baseline for the results that follow: if a structural measurement is strongly coupled with dynamics, we argue that $I_t(\mu; s)$ should be at least of order 0.1 bit, while MIs much less than this indicate weak coupling.

Figure 1 shows MI measurements between particle propensities and several aspects of liquid structure, for both KA and HS systems. Since the influence of particle type on dynamics is not directly related to glassy behavior,

we measure mutual information where the predictability based on particle type has already been taken into account. That is, we measure “the information about $\mu_{i,t}$ that is provided by a measurement s_i , for a particle whose type is already known.” In the KA system, we achieve this by restricting the distributions in (1) to particles of type A , which form the majority (80%) of the system. In the HS system, we use a conditional MI, $I(\mu; s|\alpha) = \sum_{s,\alpha} \int d\mu p(\mu, s, \alpha) \log_2(p(\mu, s|\alpha)/p(\mu|\alpha)p(s|\alpha))$, where α indicates the particle type [28]. Our choices of observable s_i reflect different theoretical pictures of glassy systems.

Low-frequency normal modes in a supercooled liquid define a set of “soft directions” on its potential energy surface (or energy landscape), and these modes influence particle dynamics [4–6,17]. Some normal mode properties can be predicted from arguments based on jamming, leading to predictions for glassy relaxation [5]. We analyze normal modes [28] by quenching the KA system to its nearest energy minimum (inherent structure), and then diagonalizing the Hessian matrix of the energy. The resulting eigenvectors and eigenvalues are \vec{v}_k and ω_k^2 , for $k = 1 \dots 3N$, and one defines a “local Debye-Waller (DW) factor” $\Delta_i^2 = \sum_k |\mathbf{v}_k^i|^2 / \omega_k^2$ that indicates [6,42] the expected size of fluctuations in the position of particle i , based on an expansion about the energy minimum. (Here \mathbf{v}_k^i is a vector containing the three components of \vec{v}_k associated with particle i .) Since low frequency modes couple most strongly to structural relaxation [6], we also define a generalized DW factor $\Delta_{i,n}^2$, which is calculated using only the n modes with lowest ω_k . In HS systems, normal modes cannot be defined by reference to a potential energy surface so we do not consider them here, although alternative definitions are possible [5,17].

Figure 1(a) shows that for relatively short time scales $t \approx \Delta t \ll \tau_\alpha$ in the KA model, the mutual information between propensity and DW factors is large (up to 0.5 bits), so Δ_i^2 and $\Delta_{i,n=150}^2$ are strongly correlated with particle

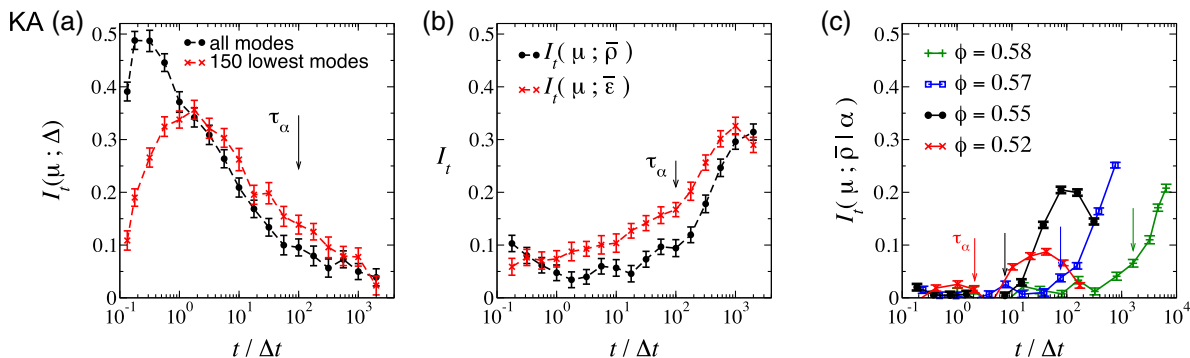


FIG. 1 (color online). MI measurements $I_t(\mu; s)$ in the KA system at $T = 0.5$, and $I_t(\mu; s|\alpha)$ in the HS system. We show MI between propensity and (a) Debye-Waller factors Δ_i and $\Delta_{i,n=150}$ in the KA system; (b) coarse-grained energy and density in the KA system; (c) coarse-grained density in the HS system. Arrows indicate the structural relaxation time τ_α and error bars indicate numerical uncertainties in the MI. In (c), the MI signals at short times are comparable with numerical uncertainties. The behavior of the MI at long times is discussed in the main text.

motion. This indicates that the normal modes accurately mimic the fluctuations of the system within its initial metastable state. On longer time scales, the MI decreases strongly: as structural relaxation takes place, the “soft directions” for further motion decorrelate from those at $t = 0$ [10,43], reducing the predictive power of the normal mode analysis. While $\Delta_{i,n=150}^2$ provides significant predictive information even at $t = \tau_\alpha$ [5,6,17], it appears that dynamical correlations on these time scales are not fully determined by motion along the “soft directions” that are present at $t = 0$. To make stronger predictions for relaxation on long time scales, one might consider correlations between successive relaxation events, for example through dynamical facilitation [15,44] or avalanches [10].

In addition to normal modes, *coarse-grained energy and density measurements* are also correlated with dynamical fluctuations [21–23,45]. In particular, field-theoretic descriptions of particle motion [18,22] are built on hydrodynamic fields such as the density. We define a local density, coarse-grained on a length scale ℓ , as $\bar{\rho}_i^\ell = \ell^{-3} \sum_j e^{-r_{ij}^2/\ell^2}$, where the sum runs over all particles j and r_{ij} is the distance between particles i and j [23]. Similarly, the locally-averaged energy is $\bar{\varepsilon}_i^\ell = \sum_j \varepsilon_j e^{-r_{ij}^2/\ell^2} / (\ell^3 \bar{\rho}_i^\ell)$ where ε_j is the energy of particle j . Figures 1(b), 1(c) show that for $\ell = 2\sigma$ these quantities have strong predictive power on time scales longer than the structural relaxation time, but the MI is smaller for times $t < \tau_\alpha$. The results are broadly similar for both models. We show data for $\ell = 2\sigma$ which illustrates the typical behavior: dependence on ℓ is discussed in Supplemental Material [28].

Throughout the glassy regime, we expect $I(\mu; \bar{\rho})$ and $I(\mu; \bar{\varepsilon})$ to have peaks at some (ℓ -dependent) time t_ℓ^* , before decreasing at longer times (see for example the HS data at $\phi = 0.55$). However, for the largest volume fractions it is clear that t_ℓ^* is significantly larger than τ_α , and exceeds our sampling window. We attribute this large time scale to hydrodynamic effects that are largely independent of glassy behavior: on general grounds we expect regions of size $\ell > \sigma$ to relax on a time scale t_ℓ^* that increases with ℓ and is significantly larger than τ_α . Relaxation in high-density or low-energy regions of size ℓ will therefore be predictably slower than average up to $t \approx \tau_\ell^*$. On these large time scales, almost all memory of the initial structure has been lost, leaving only the hydrodynamic energy or density fluctuations as the dominant predictive factor for dynamics. We argue that this effect leads to the large MI values at long times in Figs. 1(b), 1(c). In the simplest theoretical description, one expects $t_\ell^* \sim \ell^2/D$ where D is a diffusion constant; a more accurate estimate of t_ℓ^* would account for the relationship between diffusion constants and relaxation times [46,47]. However, we focus in this study on times t of order τ_α , where the system has significant dynamical heterogeneity and the motion is complex and co-operative. For the HS system, Fig. 1(c) shows that the MI at τ_α increases

at large ϕ , indicating that the coupling of dynamics to local density is increasing as the glass transition is approached, consistent with [18,22,45]. The MIs at τ_α are less than 0.1 bits for all states considered, but they increase rapidly for later times. Overall, Figs. 1(b), 1(c) show that simple observables like local energy and density couple strongly to dynamics, giving useful predictive information, particularly on relatively long time scales. We argue that these correlations merit further study, either theoretically [18] or numerically, presumably via three-point correlations [22].

Another theory of glassy relaxation is based on *locally-favored structures* (LFS): atomic or molecular packings that have low energy (or enthalpy) [14]. Particles in LFS typically have slower than average dynamics in glassy systems [7,8,48,49] and the theory [14] predicts that glassy relaxation is controlled by the formation of locally stable regions that are rich in these LFS. The LFS considered here are illustrated in Fig. 2; full details are given in the Supplemental Material [28]. For both KA and HS models, we consider an LFS that is associated with local fivefold symmetry, which we expect to be associated with lower propensity for motion [8,25,49–51]. Let $n_{155}(i)$ be the number of these structures in which particle i participates. In the KA model we also consider a particular 11-particle LFS that is correlated with slow dynamics [7,8]: we define

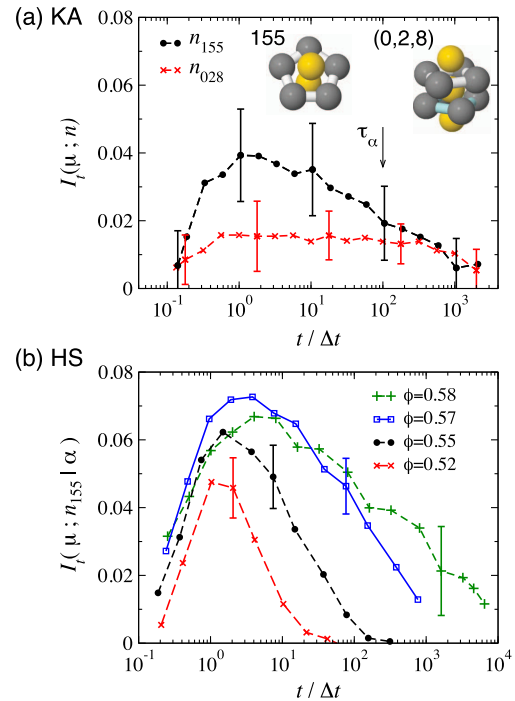


FIG. 2 (color online). MI between propensity and LFS measurements. These MIs are smaller in magnitude than those of Fig. 1, and all are less than 0.1 bit. (a) KA system, including pictures of the relevant LFS. (b) HS system, for which we consider only the ‘155’ LFS. Representative error bars are shown in (a), while (b) shows error bars only at $t = \tau_\alpha$.

$n_{028}(i) = 1$ if particle i participates in such an LFS, otherwise $n_{028} = 0$.

Figure 2(a) shows results for the KA model, indicating that n_{155} and n_{028} are correlated with particle motion [7,8]. As with the low-frequency normal modes, the MI is largest on time scales $t \approx \Delta t$ indicative of (fast) β -relaxation [1], but there is still some correlation at the structural relaxation time. However, the strength of the correlation is smaller for the LFS than for the normal modes, less than 0.1 bit in all cases. Figure 2(b) shows similar results for the HS system. Comparing the two systems, MI values are larger for the hard spheres, indicating a stronger correlation between LFS and dynamics [25]. At short times, the MI increases with increasing volume fraction. However the MI at τ_α (indicated by the error bars) depends more weakly on ϕ . We argue that the small MI values at τ_α and longer times, and the absence of an increase of the values at τ_α with volume fraction, both indicate that the LFS identified here are relatively weakly coupled to the dynamics, at least for these models and these state points [52]. In addition, the lifetimes of most LFS are less than τ_α [8,49], so their influence on dynamics is (in most cases) similarly short lived, which also limits their predictive value.

To summarize our findings so far, Fig. 1 shows that Debye-Waller factors and coarse-grained measurements of energy and density have significant coupling to dynamics, providing predictive information comparable with measurements of particle type in the KA model. The information available from LFS measurements is rather weaker. Also, the MIs for different structural measurements have very different time dependences, which we interpret in terms of the decorrelation times of the relevant structural features. These conclusions illustrate how MI measurements give useful quantitative information about causal links between structure and dynamics in these systems.

Finally, we show how information theory can also be used to analyze the predictability of particle motion, independent of any specific structural observable. Let $p_{i,t}(r)$ be the (isoconfigurational) distribution of particle displacements $r_i = |\mathbf{r}_i(t) - \mathbf{r}_i(t_0)|$. Given data for N_p particles (which may be obtained in general from many initial configurations), we define

$$I_t(r; \text{id}) = N_p^{-1} \sum_i \int dr p_{i,t}(r) \log \frac{p_{i,t}(r)}{N_p^{-1} \sum_i p_{i,t}(r)}, \quad (2)$$

which is the ‘‘average amount of information about a particle’s motion that is provided by specifying its initial environment.’’ Since a particle’s initial environment encodes all predictable aspects of its future motion, $I_t(r; \text{id})$ indicates how predictable (or reproducible) particle motion is within the system [3,23]. Figure 3 shows that $I_t(r; \text{id})$ is much larger at low temperatures in the KA model than at high temperatures, indicating that structure is more strongly coupled to dynamics at low temperatures. The relatively

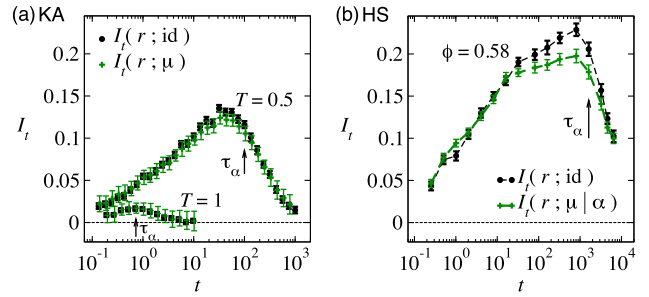


FIG. 3 (color online). Measurements of MI based on particle displacements r_i . (a) KA system for $T = 0.5$ and $T = 1$, (b) HS system at $\phi = 0.58$. See text for discussion.

small absolute values of $I_t(r; \text{id})$ are consistent with [23], and indicate that single-particle motion in glass formers has a large unpredictable component, as well as the predictable aspects that are encoded by the propensity.

It is also useful to compare $I_t(r; \text{id})$ with ‘‘the average amount of information about a particle’s dynamics that is provided by specifying its propensity,’’ which is $I_t(r; \mu) = \int dr d\mu p_t(r, \mu) \log(p_t(r, \mu)/p_t(\mu)p_t(r))$, where $p_t(r, \mu)$ is the joint distribution of displacement r and propensity μ , and $p_t(r)$ is the marginal distribution of the displacement. Since fixing a particle’s initial environment necessarily fixes its propensity, one has

$$I_t(r; \mu) \leq I_t(r; \text{id}). \quad (3)$$

From Fig. 3, the two quantities in (3) are almost equal for the KA model. Eq. (3) is an ‘‘information-processing inequality’’ [20], so this result indicates that the propensity captures almost all predictable information about single-particle displacements. For the HS system, we use a conditional MI between r and μ , to account for particle type, as above. In this case, the two MIs in (3) differ somewhat more strongly than they do in the KA model: this situation might arise (for example) if some particles have finite average displacements $\langle \mathbf{r}_i(t) - \mathbf{r}_i(t_0) \rangle$ that are only weakly correlated with their propensities.

Nevertheless, we have $I_t(r; \mu) \approx I_t(r; \text{id})$ in both models, indicating that the propensity captures almost all predictable aspects of the single-particle dynamics [3]. This further validates the MI as a measure of the influence of liquid structure on dynamics—possible generalizations of this work include the use of other structural observables s_i , or investigation of collective dynamical measurements (instead of single-particle propensities).

We thank David Chandler, Peter Harrowell, Peter Sollich, Gilles Tarjus, and Karoline Wiesner for helpful discussions. R. L. J. and A. J. D. were supported by the EPSRC through Grants No. EP/I003797/1 and No. EP/E501214/1, respectively. C. P. R. gratefully acknowledges the Royal Society for financial support.

- [1] M. D. Ediger, C. A. Angell, and S. R. Nagel, *J. Phys. Chem.* **100**, 13200 (1996).
- [2] P. G. Debenedetti and F. H. Stillinger, *Nature (London)* **410**, 259 (2001).
- [3] A. Widmer-Cooper, P. Harrowell, and H. Fynewever, *Phys. Rev. Lett.* **93**, 135701 (2004); A. Widmer-Cooper and P. Harrowell, *J. Chem. Phys.* **126**, 154503 (2007).
- [4] D. Coslovich and G. Pastore, *Europhys. Lett.* **75**, 784 (2006).
- [5] C. Brito and M. Wyart, *J. Stat. Mech.* (2007) L08003.
- [6] A. Widmer-Cooper, H. Perry, P. Harrowell, and D. R. Reichman, *Nat. Phys.* **4**, 711 (2008).
- [7] D. Coslovich and G. Pastore, *J. Chem. Phys.* **127**, 124504 (2007).
- [8] A. Malins, J. Eggers, H. Tanaka, and C. P. Royall, *Faraday Discuss.* **167**, 405 (2013).
- [9] M. Leocmach and H. Tanaka, *Nat. Commun.* **3**, 974 (2012).
- [10] R. Candelier, A. Widmer-Cooper, J. K. Kummerfeld, O. Dauchot, G. Biroli, P. Harrowell, and D. R. Reichman, *Phys. Rev. Lett.* **105**, 135702 (2010).
- [11] V. Lubchenko and P. G. Wolynes, *Annu. Rev. Phys. Chem.* **58**, 235 (2007).
- [12] J.-P. Bouchaud and G. Biroli, *J. Chem. Phys.* **121**, 7347 (2004).
- [13] W. Götze and L. Sjögren, *Rep. Prog. Phys.* **55**, 241 (1992).
- [14] G. Tarjus, S. A. Kivelson, Z. Nussinov, and P. Viot, *J. Phys. Condens. Matter* **17**, R1143 (2005).
- [15] J. P. Garrahan and D. Chandler, *Proc. Natl. Acad. Sci. U.S.A.* **100**, 9710 (2003); D. Chandler and J. P. Garrahan, *Annu. Rev. Phys. Chem.* **61**, 191 (2010).
- [16] T. Kawasaki, T. Araki, and H. Tanaka, *Phys. Rev. Lett.* **99**, 215701 (2007).
- [17] M. L. Manning and A. J. Liu, *Phys. Rev. Lett.* **107**, 108302 (2011).
- [18] G. Biroli, J. P. Bouchaud, K. Miyazaki, and D. R. Reichman, *Phys. Rev. Lett.* **97**, 195701 (2006).
- [19] M. D. Ediger, *Annu. Rev. Phys. Chem.* **51**, 99 (2000).
- [20] T. M. Cover and J. A. Thomas, *Elements of Information Theory* (Wiley, New York, 1991).
- [21] G. S. Matharoo, M. S. Gulam Razul, and P. H. Poole, *Phys. Rev. E* **74**, 050502 (2006).
- [22] L. Berthier, G. Biroli, J.-P. Bouchaud, W. Kob, K. Miyazaki, and D. R. Reichman, *J. Chem. Phys.* **126**, 184503 (2007).
- [23] L. Berthier and R. L. Jack, *Phys. Rev. E* **76**, 041509 (2007).
- [24] W. Kob and H. C. Andersen, *Phys. Rev. E* **51**, 4626 (1995); **52**, 4134 (1995).
- [25] C. P. Royall, A. Malins, A. J. Dunleavy, and R. Pinney (to be published).
- [26] L. Berthier and W. Kob, *J. Phys. Condens. Matter* **19**, 205130 (2007).
- [27] M. N. Bannerman, R. Sargant, and L. Lue, *J. Comput. Chem.* **32**, 3329 (2011).
- [28] See Supplemental Material at <http://link.aps.org/supplemental/10.1103/PhysRevLett.113.095703> for details, which includes Refs. [29–35].
- [29] A. Malins, S. R. Williams, J. Eggers, and C. P. Royall, *J. Chem. Phys.* **139**, 234506 (2013).
- [30] For a review, see K. Hlavackova-Schindler, M. Palus, M. Vejmelka, and J. Battacharya, *Phys. Rep.* **441**, 1 (2007).
- [31] T. Schürmann and P. Grassberger, *Chaos* **6**, 414 (1996).
- [32] I. Nemenman, F. Shafee, and W. Bialek, in *Advances in Neural Information Processing Systems* Vol. 14, edited by T. G. Dietterich, S. Becker, and Z. Ghahramani (MIT Press, Cambridge, MA, 2002).
- [33] A. Kraskov, H. Stögbauer, and P. Grassberger, *Phys. Rev. E* **69**, 066138 (2004).
- [34] M. B. Kennel, J. Shlens, H. D. I. Arbanell, and E. J. Chichilnisky, *Neural Comput.* **17**, 1531 (2005).
- [35] E. Archer, I. M. Park, and J. W. Pillow, *Entropy* **15**, 1738 (2013).
- [36] D. Chandler, *An Introduction to Modern Statistical Mechanics* (Oxford University Press, New York, 1987).
- [37] J. Kurchan and D. Levine, *J. Phys. A* **44**, 035001 (2011).
- [38] A. J. Dunleavy, K. Wiesner, and C. P. Royall, *Phys. Rev. E* **86**, 041505 (2012).
- [39] C. Cammarota and G. Biroli, *Europhys. Lett.* **98**, 36005 (2012).
- [40] T. Aste, P. Butler, and T. Di Matteo, *Philos. Mag.* **93**, 3983 (2013).
- [41] P. Ronhovde, S. Chakrabarty, D. Hu, M. Sahu, K. K. Sahu, K. F. Kelton, N. A. Mauro, and Z. Nussinov, *Eur. Phys. J. E* **34**, 105 (2011); *Sci. Rep.* **2**, 329 (2012).
- [42] A. Widmer-Cooper and P. Harrowell, *Phys. Rev. Lett.* **96**, 185701 (2006).
- [43] S. S. Schoenholz, A. J. Liu, R. A. Riggleman, and J. Rottler, [arXiv:1404.1403](https://arxiv.org/abs/1404.1403).
- [44] A. S. Keys, L. O. Hedges, J. P. Garrahan, S. C. Glotzer, and D. Chandler, *Phys. Rev. X* **1**, 021013 (2011).
- [45] L. Berthier, G. Biroli, J.-P. Bouchaud, L. Cipelletti, D. El Masri, D. L'Hôte, F. Ladieu, and M. Pierno, *Science* **310**, 1797 (2005).
- [46] Y. J. Jung, J. P. Garrahan, and D. Chandler, *Phys. Rev. E* **69**, 061205 (2004).
- [47] P. Chaudhuri, L. Berthier, and W. Kob, *Phys. Rev. Lett.* **99**, 060604 (2007).
- [48] C. P. Royall, S. R. Williams, T. Ohtsuka, and H. Tanaka, *Nat. Mater.* **7**, 556 (2008).
- [49] A. Malins, J. Eggers, C. P. Royall, S. R. Williams, and H. Tanaka, *J. Chem. Phys.* **138**, 12A535 (2013).
- [50] H. Jonsson and H. C. Andersen, *Phys. Rev. Lett.* **60**, 2295 (1988).
- [51] J. D. Honeycutt and H. C. Andersen, *J. Phys. Chem.* **91**, 4950 (1987).
- [52] G. M. Hocky, D. Coslovich, A. Ikeda, and D. R. Reichman, [arXiv:1402.6709](https://arxiv.org/abs/1402.6709).